Insole customized Part 1: Non-contact Method of Anthropometric points Detection for Feet

Maneesh Kumar Mishra[1, 2, 3]**, Pascal Bruniaux**[1, 2, 3]**, Guillaume Tartare**[1, 2, 3] **and Christine Campagne**[1, 2, 3]

[1] **University of Lille Nord de France, Lille, France**

[2] **Ecole Nationale Supérieure des Arts et Industries Textiles, Roubaix, France**

[3]**GEMTEX, Roubaix, France**

E-mail: maneesh09mishra@gmail.com, maneesh.mishra@ensait.fr

Abstract

Regardless of the objectives of the study, whether it is the morphological classification of the feet or the customization of products such as orthopedic insoles or appropriate footwear for atypical feet, it is the imperative to find a rational method for detecting the anthropometric points and curves. The studies explaining the anthropometry of the foot are very few and in some cases present contradictions in the measurements between the manual and automatic scanning processes. In addition, our goal was to implement a non-contact measurement method to detect the anthropometric points of feet. This method proposes different tracking techniques using different adjustable planes. In a 3D graphical process, the morphological curves have been located with the help of these anthropometrics points and allowed the identification of the foot by their measurements. These measurements were compared with those obtained by a 3D foot scanner to validate the detection method of anthropometric points and improve it by employing these scanners.

Keywords

3D graphical process, 3D insole model, foot morphology, foot anthropometry, customized insole.

1. Introduction

As a complex structure, the human body can be divided into five parts: the head, the neck, the torso, two arms extended by hands and two legs extended by feet. Every organ has its own unique function. For example, the feet carry the weight of the body in standing position and allow walking and running.

Foot anatomy is very complex, matching the complexity of the tasks it needs to perform. One foot is composed of 42 muscles, 26 bones, 33 joints, and at least 50 ligaments and tendons made of strong fibrous tissue to keep all the moving parts together, as well as 250,000 sweat glands. This evolution wonder is able to support hundreds of tons, representing our weight in motion each day. The innumerable parts of the foot work in harmony to bring us from one place to another. However, the stress and the constraints of movements expose them to a greater risk of injury than other body parts, depending on our overall anatomy. It is therefore important to know the different pathologies of feet to avoid them a priori or treat them a posteriori. Of course, an anthropometric knowledge of the foot and various tools of measurement are necessary for the diagnosis of a podiatrist, the design of the shoe which protects it or which contributes to the treatment of certain pathologies. Many of these diseases stand in correlation with the design of particular shoes or insoles. Regardless of whether there is a need for personalization of the products, the knowledge of the morphology and foot dimensions should be spread through measurement campaigns.

Many foot problems, including hammertoes, blisters, bunions, corns and calluses, heel spurs, claw and mallet toes, ingrown toenails, toenail fungus and athlete's foot, can develop due to neglect, ill-fitting shoes or and simply tear and wear. Feet can also indicate if the body is under threat from a serious disease. Gout, for instance, will attack the foot joints first.

A hammertoe is a condition in which the second, third, or fourth toe is crossed, bent in the middle of the toe joint, or just pointing at an odd angle. Hammertoes are often caused by ill-fitting shoes. Women are more prone to suffer pain associated with hammertoes than men because of different kinds of fancy footwear and shoe gear. Since the muscles of each toe work in pairs, when the toe muscles get out of balance, a hammertoe can form [1][2]. Due to this muscle imbalance, the toe's tendons and joints suffer a lot of pressure which forces the toe into a hammerhead shape. Hammertoe hazards include flat feet, high arch, genetic causes, arthritis, toe injury and aging. Hammertoes can become a serious problem for people with diabetes or poor blood circulation, as they are under a higher risk of infections and foot ulcers [3].

A bunion is a crooked big-toe joint (hallux valgus) that protrudes at the base of the toe, forcing the big toe to turn inwards. A bunion can be painful when confined in a shoe, and for many people, shoes that are too narrow in the toe region may lead to the formation of bunions [4][5]. Studies reported that individuals with hallus valgus have lower thickness and cross-sectional area of abductor halluces and flexor halluces brevis, compared to individuals without hallux valgus [6]. Generally, hallux valgus is caused by various factors, including inborn deformities, arthritis, trauma, and heredity [7]. It has been suggested that atrophied or weak toe flexor muscles are associated with the formation of toe deformities. However, there is not enough evidence to support this theory. Nevertheless, high heels (forcing toes into the front of shoes), ill-fitting shoes (too tight, too narrow or too pointed shoes make feet more susceptible to bunions) may increase the likelihood of suffering this deformity [8]. Therefore, strengthening the intrinsic toe muscles may help reduce the incidence and severity of toe deformities in older adults [9]. Shoes and insoles need to conform to the wearer's foot shape without squeezing or pressing any part of the foot [10].

Plantar fasciitis is acknowledged as synonym of inflammation of the plantar fascia and the suffix "-itis" integrally suggests an inflammatory disease. It is common for doctors to confuse heel spurs and plantar fasciitis

when a patient comes in for heel pain. Heel spurs are found in 70 percent of patients with plantar fasciitis, but these are two different conditions [11][12]. The heel spurs themselves are not painful; it is the inflammation and irritation caused by plantar fasciitis that can hurt. Heel spurs are often observed on X-rays of patients who do not feel heel pain or plantar fasciitis [13]. Almost 10 percent of injuries occur among athletes whose activities include frequent running and jumping [14].

There are basically two kinds of arches: longitudinal arches (consisting of medial and lateral parts, distributing body weight and pressure in different directions together with transverse arches) and transverse arches [15]. According to the research conducted by Subotnick, 60% of the population have normal arches, 20% have a cavus foot (high arch), and 20% have a planus foot (low arch) [16]. When longitudinal arches are higher than normal, this is termed as high arch [17][18]. It has an imprint with or without a narrow band connecting the forefoot and the heel region. The bony (over-supinated) structure on the lateral side of the foot is at higher risk of injury due to smaller area bearing the weight, thereby transmitting higher stresses to the foot and leg. A neurologic syndrome and other medical conditions often cause high arch (Cavus foot), e.g. cerebral palsy, Charcot-Marie-Tooth disease, spina bifida, polio, muscular dystrophy, or stroke.

When longitudinal arches are low, this is referred to as planus foot [19][20]. Planus foot, like cavus foot, does not transmit forces efficiently and therefore may lead to foot ache. Moreover, this also affects proper pressure distribution in other parts of body, which may cause back pains in long term. This metamorphosis is the result of a greater inversion of the rear foot that occurred at heel strike in the low-arched group [21].

Birtane et al. evaluated the effects of different obesity categories on the plantar pressure values [22]. Their study examined the feet (left and right) of 50 participants classified as non-obese and class one obese, according to their body mass index values. Examined pressure zones were as follows: peak phalanx pressure, medial forefoot peak pressure, middle forefoot peak pressure, lateral forefoot peak pressure, middlefoot peak pressure, rearfoot peak pressure, plantar contact area.

Veal et al. quantified the weight increase [23]. The authors examined whether the increase in weight had an impact on the mean peak foot pressures by controlling the foot function, deformity, and structure. Novel's in-shoe dynamic pressure measuring system (Pedar system) has been used to measure peak plantar foot pressures.

This part presents the main diseases and pathologies of the foot. Pathological assessments show that the knowledge and analysis of the morphology and anthropometry are decisional factors in the diagnosis of a podiatrist.

2. Morphological analysis

Morphological analysis is a domain related to the proportion and dimensions of anthropometric measures. Morphological knowledge is important in several domains because it can explain e.g. the cause of physiological ailments. The prominence of anthropometry has been playing a vital role in forensic research, in terms of identifying the victim's sex, population group and demographics [24]. In the footwear industry, anthropometry has been an important tool for optimizing shoe and insole shapes according to different age groups, races, body composition and gender specifics. Many papers attempt to tackle the optimization problem and are connected to measurement campaigns. There are several basic methods of foot measurement available on the market, such as caliper ruler, blueprints, tape measures, etc. However, contemporary methods such as 3D foot-scanners appear more suitable. The plaster cast is a convenient and cost-effective method, often used by orthopaedists to obtain the 3D shape of the foot. However, 3D scanners prove more appropriate, cost-efficient and applicable for the creation of client database or measurement campaigns.

Our priority is to analyze 3D feet anthropometry, to examine state-of-art methods of foot measurement and to verify or define the correlation between them.

2.1. Anthropometry of the foot

By definition, anthropometry is the measurement technique of the human body and its various parts. The measurement of a human body is strongly related to different anthropometric points defined by the bones [25]. **Figure 1** shows different bones of the foot; the anthropometric points visible from this point of view are marked red and green as an example.

In the case of scanning an entire human body, different planes (sagittal, frontal, transverse) partition it in order to prepare the measurement process [26], which is not the case with the feet. In the works of Witana et al. [27], the anthropometric points are the only measurement references which have been used to classify 18 dimensions by categories, according to the length between the two points and a plane, the width between two points and the girth of contours positioned with respect to one, two or three points. These 18 categories are as follows: foot length, arch length, heel to medial malleolus, heel to lateral malleolus, heel to fifth toe, foot width, heel width, bimalleolar width, mid-foot width, medial malleolus height, lateral malleolus height, height at 50% foot length, ball girth, instep girth, long heel girth, short heel girth, ankle girth, waist girth.

To compare foot dimensions between the two genders and the corresponding data from other populations, Hajaghazadeh et al. have added others dimensions [28]. Lengths of the second, third and fourth toe measured in the direction of the Brannock Axis have been added to obtain 21 dimensions in total.
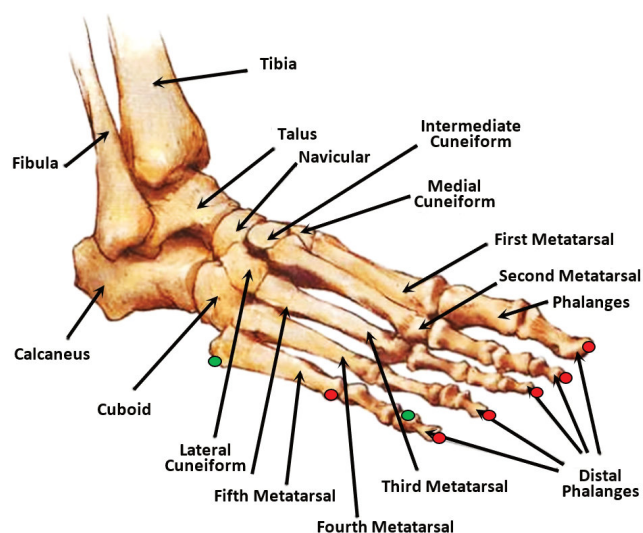
Figure 1: Different bones of foot. Anthropometric points.

2.2 Foot measuring techniques

Manufacturing comfortable footwear relies on anthropometric research, which determines the morphological character of the foot, the functioning of the foot-footwear system and the results of the morpho-functional optimization of the shape of the product. Natural anatomic-morphological constructions of the foot and its correct static and dynamic functioning are ensured by a rational inner shape of the shoe, determined by the construction of the shoe last. The construction of the shoe last and the establishment of the dimensions necessary to meet the comfort requirements of a larger proportion of consumers with minimal production costs must be based on knowledge and the most accurate characterization of anatomic morphological differences between foot types frequently encountered within the targeted consumer population. For this purpose, it is necessary to periodically perform anthropometric studies of the population according to certain criteria (sex, age, geographical region, etc.), in order to obtain information about the dimensional particularities of the average representative foot for that population, i.e. the laws of distribution of anthropometric parameters that characterize the representative average foot of the population of the respective country [29].

The most common approaches include the use of digital calipers for direct measurements and 3D scanning and footprint analysis for indirect measurements. It is very important to provide adequate training for the technicians to correctly position landmarks on the proper anatomical points.

The main objective of taking measurements of the human foot is to determine the most precise dimensions of the foot, which enables the design of the shoe last, which is the physical support essential to shoe design.

Traditional measurement methods, e.g. the ink footprint, digital caliper and Brannock Device are the traditional manual approaches used to determine foot dimensions. However, the accuracy of digital caliper measurement tends to be affected by human error. Different technicians may obtain inconsistent measurement results. It is very important to provide adequate training for the technicians to correctly position landmarks on the proper anatomical points [30]. Furthermore, it is necessary to respect the rules and norms to obtain measurements with reliable results [31]. Other means of traditional measurements measure the length of the correctly oriented foot, the strategic angles and anthropometric contour girths, correctly identified with respect to the anthropometric points.

The Digital Caliper (sometimes incorrectly called the Digital Vernier Caliper) is a precision instrument that can be used to measure internal and external distances extremely accurately. McPoil et al. used the digital calipter to measure and combine several anthropometric measurements to predict the plantar surface [32]. The six measures that were considered in the study are as follows: total foot length, ball length, dorsal arch height, forefoot width, midfoot width, heel width.

Designed in 1927, the Brannock Device is a foot-measuring device which has become a must in all retail footwear stores. Measuring accuracy, quality construction, and simple, yet completely functional manually operated design have made genuine Brannock measuring devices the standard in the footwear industry [27]. Although this measurement instrument is considered among the most reliable in measuring the lengths of the foot given its perfect alignment with the Brannock axis, some authors still use the traditional measuring tape in their measurement campaigns [33][34]. These techniques somewhat lack up-to-the-mark precision in obtaining measurement which could be used for atypical morphologies.

3D digital measurement is usually performed with a 3D scanner of different types, depending on the desired measurement height. The company BFTS Human Technology offers two versions of INFOOT 3D scanner [35]. The first version can measure a height of 150mm, while the second version measures up to 250mm. The advantage of the second product comes into play in boot design, which requires a deeper knowledge of the upper part of the foot, or in the sector of orthosis. The 3D foot scanner uses the optical laser scanning technology. INFOOT scans a foot form from the anatomical landmark points, and automatically measures almost 20 measuring items as maximum.

Witana et al. show a great interest in using the 3D foot scanner. In their study, the authors have compared the measurement results of a 3D scanner with manual foot measurements. Their work highlights important differences in measurement accuracy from the abovementioned measurement tools, along with the measuring protocol, measuring time and skill level of the measurer [27]. Lee et al. have also achieved similar results by comparing the scanner to conventional foot measurement methods, in particular the digital caliper, ink footprint, and digital footprint [30]. The 3D scanner has been an indispensable tool for the evaluation of anthropometric parameter results obtained by 3D measurements and their statistical and mathematical processing in the works of Pantazi et al. [29]. The 3D foot scanner has also been used by Nácher et al. for its accuracy and rapidity in classifying the feet of a population of 316 female participants. The aim of this study is to improve the comfort of shoes by designing a model for predicting footwear fit on the basis of processed data [36].

In the podiatry sector, other techniques are used to directly obtain the 3D form of the underside shape of the foot in creating orthopedic insoles adapted to the patient. One example is the box with double imprint [37] that allows the realization of the 3D shape of the two feet in plaster or resin and the design of orthopedic insoles. This manual technique is not expensive but requires expertise in molding and the creation of the insole. This process could be conducted numerically and more quickly in CAD.

Manual measurement generally leads to measurement errors, depending on the operator and their fatigue if the measuring is performed on many people. To avoid this type of problem, the industry has developed different types of the 3D foot scanner. However, the measurement protocol and the exploitation of the results of these new foot measurement tools can affect the precision of the measurements. Therefore, this paper intends to implement own measurement method based on the 3D raw data of the scanner. These measurements will be compared with those obtained directly by the software sold by the manufacturer of the selected scanner. An anthropometric analysis is necessary because it represents the core of the measurement process.

3. Anthropometric analysis and feet measurements

3.1. Anthropometric points

Foot measurements depend essentially on the anthropometric points defined in precise places of its skeleton. The manual foot measurement instrument, which is used and validated scientifically, is a device that was invented by Brannock. The positioning of the foot in this instrument makes it possible to define a reference axis for the measurements, i.e. the Brannock axis. As a general rule in case of a foot that does not have a deformation problem (typical deformation as an indicator of diseases), the reference axis is a virtual line between pternion and the tip of the second toe (A). Since there may be slight differences between measurements obtained manually using a tape measure, Brannock's instrument and a 3D scanner, it seems important to recall the anthropometric points which are essential for foot measurement and the way these measures should be taken or interpreted, in order to find the best compromise between these different methods. 19 anthropometric points which are recognized today are as follows:

1) Pternion :

2) Metatarsal tibiale : Most medially prominent point on the 1st metatarsal bone

3) Medial malleolus : Most medial point of medial malleolus

4) Lateral malleolus : Most lateral point of lateral malleolus

5$_n$) Toe n^{th} : n^{th} toe tip

6) Instep: Top of instep point

7) Metatarsal fibulare : Most laterally prominent point on the 5th metatarsal bone

8) Highest point of 1st metatarsal : Top of ball girth point

9) Sphyrion :

10) Sphyrion fibulare :

11) Landing point : Back heel point

12) Junction point :

13 & 13') Calcaneum points : Most medially and laterally prominent points on the calcaneum bone

14) Navicular :

15) 5th metatarsal : Tuberosity of 5th metatarsal

16) Toe 1st joint : Highest point of Toe 1st joint

17) Toe 5st joint : Highest point of Toe 5st joint

18) 1st metatarsal : Highest point of 1st metatarsal head

19) Mid-foot highest point : Highest point of the vertical girth at 50% foot length from the pternion

Figure 2 shows the position of these points in relation to the foot skeleton and the joints. In practice, these points will be positioned with a slight shift caused by the muscular surplus that surrounds the bone structure.
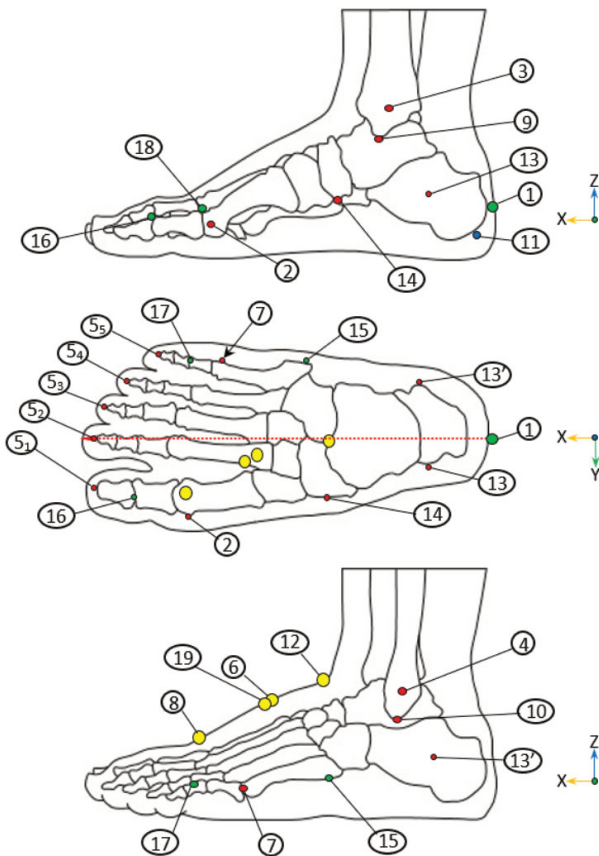
Figure 2: Anatomical bones, anthropometric points.

3.2 Feet measurements

Foot measurements are generally classified into 4 categories (lengths, heights, widths, and girths). The fifth category (angles) required for the design of footwear products (sole, shoe) is derived from the previous measurements:

Lengths: The whole distances are measured along the Brannock axis (X-direction)

L1 - Foot length: distance from point 1 to the tip of the longest toe.

L2 - Arch length: distance from point 1 to point 2.

L3 - Heel to medial malleolus: length from point 1 to point 3

L4 - Heel to lateral malleolus: length from point 1 to point 4

L5 - Heel to fifth toe: distance from point 1 to point 5.

L6 - Heel to Sphyrion: distance from point 1 to point 9.

L7 - Heel to Sphyrion fibulare: distance from point 1 to point 10.

Heights: The whole distances are measured in the vertical direction (Z-direction)

H1 - Medial malleolus height: distance from the floor to point 3.

H2 - Lateral malleolus height: distance from the floor to point 4.

H3 - Height of instep: distance from the floor to point 6.

H4 - Sphyrion height: distance from the floor to point 9.

H5 - Sphyrion fibulare height: distance from the floor to point 10.

H6 - Mid-foot Height: Maximum height measured with a line at 50% of foot length from point 1

Widths: The whole distances are measured in the direction perpendicular to the Brannock axis (Y-direction). Errors may occur with this type of measurement, because these distances may be the shortest distance between the measuring points in manual mode with a cephalometer or with some 3D scanners.

W1 - Foot width: distance from point 2 to point 7

W2 - Bimalleolar width: distance from point 3 to point 4

W3 - Mid-foot width: Maximum breadth measured with a line at 50% of foot length from point 1.

W4 – Heel width: distance from point 13 to point 13'

Girths: This type of measurement can represent the contour drawn on the shape (e.g. scanner or CAD) or an equivalent contour representative of a stretched tape measure.

G1 - Ball girth: Girth of foot passing through point 2, point 8 and point 7.

G2 - Instep girth: Smallest girth passing through point 6.

G3 - Long heel girth: Girth of foot passing through point 6 and point 11.

G4 - Short heel girth: Minimum girth passing through point 12 and point 11.

G5 - Ankle girth: Horizontal girth passing through point 12.

G6 – 50% foot length girth: Vertical girth at 50% foot length from point 1.

Angles: Angle according to the sideline of the foot (plane B and subsequently C)

A1 - Toe 1st angle: Angle with the plan B.

A2 - Toe 5th angle: Angle with the plan C.

3.3 Measurement protocol for 3D foot scanner

The first measurement campaign was carried out to start developing a sufficient database to validate our 3D graphical process. Feet of one hundred people were scanned. No distinction was made between the feet of women and men. At this stage of the study, the morphology of the feet does not depend on sex. The distinction will be made only later in the construction of footwear according to the population targets envisaged by the industry sector (i.e. the footwear industry).

The measuring device that has been used to scan the different feet in our database is the foot scanner of INFOOT society. The measurement protocol is imposed by the designer. In the first phase, 8 patches must be glued on the foot of the scanned person so that the software can size the overall volume of the foot (**Figure 2**).

A tactile analysis of the bones of the foot is carried out in order to better detect the following anthropometric points: metatarsal fibulare 7, sphyrion fibulare 10, lateral malleolus 4, instep 6, metatarsal tibiale 2, navicular 14, sphyrion 9, and medial malleolus 3 (**Figure 3**).

Five red stickers localize the points of reference for the calculation of different anthropometric points and the positioning of morphological contours. Anthropometric reports on which the user can intervene contribute to the automatic calculation process and its calibration if needed. **Figure 3** shows the result obtained on the tested morphology.

Figure 3: Landmarks for the scan process.
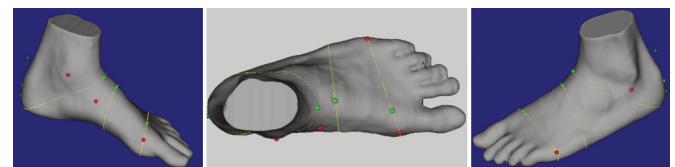
Figure 4: Detection of anthropometric points and morphological curves on real foot.

Figure 5 shows the results of measurements (lengths, widths, heights, angles and girth) taken under normal conditions of use of the scanner, i.e. the feet must be positioned between the two green lines.
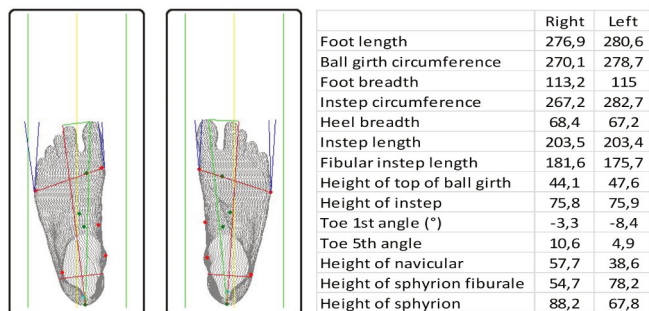
Figure 5: Scan and measurements of feet.

	Right	Left
Foot length	276,9	280,6
Ball girth circumference	270,1	278,7
Foot breadth	113,2	115
Instep circumference	267,2	282,7
Heel breadth	68,4	67,2
Instep length	203,5	203,4
Fibular instep length	181,6	175,7
Height of top of ball girth	44,1	47,6
Height of instep	75,8	75,9
Toe 1st angle (°)	-3,3	-8,4
Toe 5th angle	10,6	4,9
Height of navicular	57,7	38,6
Height of sphyrion fiburale	54,7	78,2
Height of sphyrion	88,2	67,8

4. 3D graphical process

This chapter discusses the implementation of a new method of foot anthropometry. It is a very precise method that is applicable, or even adaptable to each foot because it is semi-automatic, i.e. it is commandable with a set of parameters specific to the morphology of the patient or client. Each step of the process must be rigorously followed, given the anthropometric links integrated into the process.

4.1 Outline encompassing the footprint

The first step of the 3D graphical process is to wedge the foot in a trapezoid composed of six planes to define the geometry of the optimal outline encompassing the footprint. Two techniques are used in order to acieve this and their goal is to find the contact area or areas between the plane perpendicular to the ground and the 3D shape of the foot.

As this is performed manually during the measurement of the foot, it is essential to first wedge the heel on the vertical plane A to define the zero of the coordinate system along the X axis, which allows to detect the contact zone, providing an approximation of the position of point 1, called 1' (**Figure 2** & **Figure 6a**). Then the foot is translated and turned so that it is stuck on the vertical plane-B to the plane-A, which leads to two contact zones. In our process, the procedure is reversed since the foot is fixed and spotted in the absolute coordinate system R0(O,x,y) (**Figure 6a**). It is necessary to look for the plane-B before the plane-A. A movable coordinate system R1(O1,x,y) is therefore designed in relation to R0 and controlled by two translations along the X and Y axes and a rotation along the Z axis. Two lines aligned on the X and Y axes of R1 supporting the two planes will be able to translate and rotate so that the areas can be visualized by their associated planes.
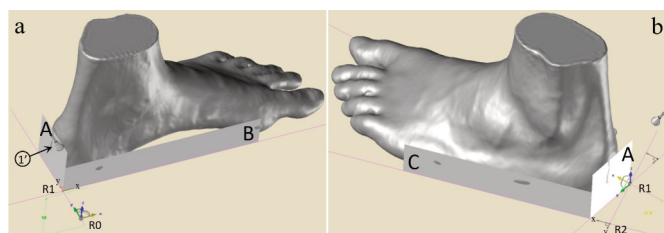
Figure 6: Wedging the heel by two planes, detection of medial and lateral contact points.

In the same way, plane-C has been positioned by a movable coordinate system R2(O2,x,y) (**Figure 6b**). This coordinate system is designed relative to R1 and controlled by a translation along the Y axis and a rotation along the Z axis. The line aligned on the X axis of R2 supporting the plane will translate and rotate so that it can be visualized the two zones by its associated plane.

The plane-D enables the search for the angle of inclination of the first toe. It is positioned by a movable coordinate system R3(O3,x,y), whose origin O3 slides by translation on the line representing the Y axis of R1 (**Figure 7a**). The coordinate system R3 pivots about its Z axis to manage the angle of inclination of its X axis, on which the line supporting the detection plane of the contact zone with the foot is aligned.

The plane-E looks for the angle of inclination of the fifth toe (**Figure 7b**). It is positioned by a movable coordinate system R4(O4,x,y), whose origin O4 slides by translation on the line representing the Y axis of R1. The coordinate system R4 pivots around its Z axis to manage the angle

of inclination of its X axis, on which the straight line supporting the detection plane is aligned.
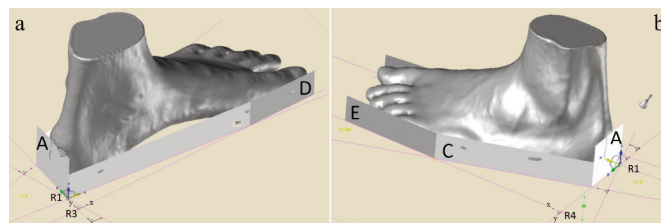
Figure 7: Detection of medial and lateral contact points of toes.

At this point in the process, it is required to locate the Brannock axis. In the first phase, a median axis between the two planes-B and C is created to detect the point of intersection B_1 between this axis and the line associated with the plane-A (**Figure 8a**). This point is the starting point B_1 of the Brannock axis, because it represents the projection of the anthropometric point 1 (re-adjustment of point 1') on the ground.
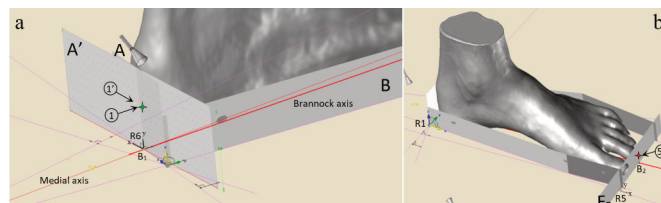
Figure 8: Detection of contact points 1, 5_2; creation of Brannock axis.

The other end is located at the end of the second toe (**Figure 8b**). The detection of this end goes through the creation of a movable coordinate system R5(O5,x,y), whose origin O5 slides by translation on the line representing the X axis of R1. The reference R5 pivots about its Z axis to manage the angle of inclination of its Y axis on which the line supporting the detection plane F2is aligned. This angle must be adjusted so that the plane F_2 is perpendicular to the Brannock axis. Once the endpoint 5_2 is found, it projects on the right, representing the Y axis to create the second end B_2 of the Brannock axis. This axis can then be plotted from B_1. Then, a new coordinate system R6(O,x,y) on the point B_1 is created perpendicular to the Brannock axis (**Figure 8a**). A detection plane A' is created from the line representative of the X axis of R6 in order to readjust the final position of point 1. The condition is that point 1 must be at the same height as in the area detected by A'.

The outline encompassing the footprint can now be finalized by creating the last F_1 plane that detects the 5_1 end of the first toe (**Figure 9a**). This plane is aligned on the line representing the Y axis of a coordinate system R7(O7,x,y), whose origin O7 translates on the Brannock axis. Among other things, the Y axis of this coordinate system is perpendicular to the Brannock axis. **Figure 9b** shows the detected contour which enables the location of anthropometric points.
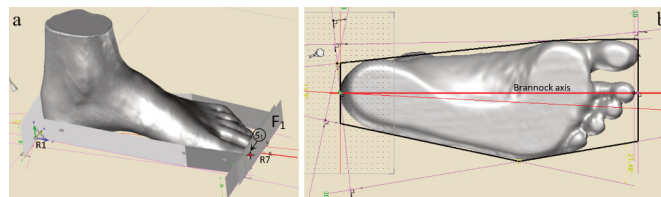
Figure 9: Detection of contact point 5_1, outline encompassing the footprint.

4.2 Detection and measurement of anthropometric points

Toes tip (5_1, 5_2, 5_3, 5_4, 5_5)

As with the first toe, different coordinate systems R8(O8,x,y) R9(O9,x,y) R10(O10,x,y) have been placed along the Brannock axis to create different lines representing the Y axis of each coordinate system (**Figure 10a**). Detection plans F_3, F_4, F_5 were created on each line (**Figure 10b**). The three end points 5_3, 5_4, 5_5 of the last toes detected by these planes are then projected onto the Brannock axis. The length of each toe with respect to B_1 (projected from 1) can be measured directly on X axis of the coordinate systems of 5_1, 5_2, 5_3, 5_4, 5_5.
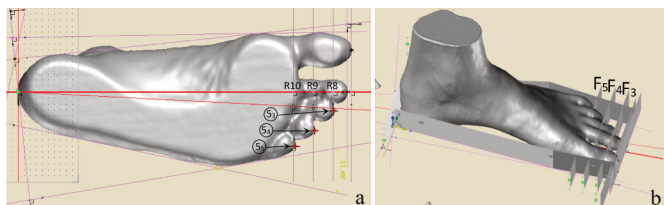
Figure 10: Detection of contact points $5_3, 5_4, 5_5$.

Junction point (12) and landing point (11)

The junction point is defined from two inclined planes, plane G in the oblique direction of the top of the foot (in side view), and plane H in the direction of the contact zone of the lower part of the tibia (in side view) (**Figure 11a**). These two planes are perpendicular to the plane B and are created from two lines: one oriented along the X axis of coordinate system R11(O11,x,y) and the other oriented along the Y axis of coordinate system R12(O12,x,y) (**Figure 11c**). These coordinate systems rotate around the Y axis of R1 in the XY plane of R1 in order to respect the perpendicularity. The orientation of these coordinate systems and their relative position with respect to the reference R1 make it possible to manage the zones of tangency of the planes in contact with the foot.

Then, a coordinate system R13(O13,x,y) is created at the intersection of the two lines defining the contact planes G and H. This coordinate system has a Y axis aligned with the X axis of R11. A cylinder is then created and centered at O13, its main axis being aligned on the Z axis of R13 (**Figure 11b**). The Z axis of R13 is also at the intersection of the two planes G and H. By modifying the diameter of this cylinder, the contact zone of the heel representing the landing point 11 can be detected.
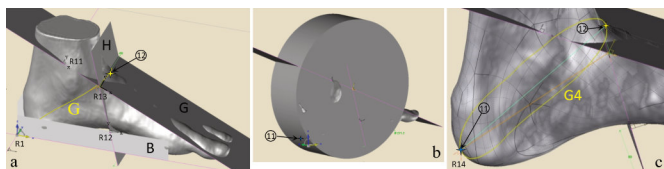
Figure 11: Detection of contact points 11, 12.

A cutting coordinate system R14(O14,x,y) is create from a straight line connecting the origin point O13 of R13 and the landing point 11 that has been positioned and directed on the point 11 (**Figure 11c**). The yellow curve resulting from the section of the foot by the cutting plane of R14 represents the short heel girth G4. The junction point 12 is at the extremum of this curve in a vertical direction upwards.

Instep point (6)

The instep point 6 is a point detected with the plane G. It is located in the lower part of the contact zone (**Figure 12a**). This point is one of the three passage points of the curve of the instep girth G2. The second point A_{rs} is located at the upper part in the arch (**Figure 12a**). The intersection between the plane B1 parallel to B and the foot makes it possible to create a portion of the curve symbolizing the shape of the internal arch. The third point B_{mid} is defined in the middle of two points B_{max}, B_{min}, located at the ends of the tangent areas of the plane C. These points are defined on the creation line of the plane G (**Figure 12a**). Since the B_{mid} point does not belong to the surface of the foot, it is required to create a R15(O15,x,y) cut mark on 6 to create the G2 curve. The curve G'2 is a curve perpendicular to the Brannock axis, representing the instep girth G'2 proposed by the foot scanner.
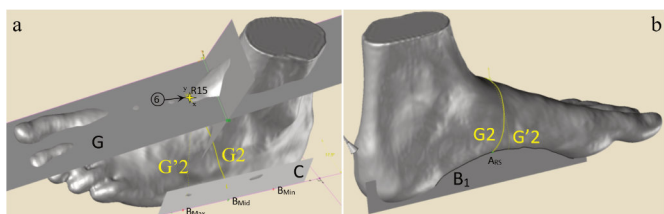
Figure 12: Detection of contact point 6.

Metatarsal tibiae (2), metatarsal fibulae (7), highest point of 1st metatarsal (8)

The metatarsal tibial point 2 and metatarsal fibular point 7 can be detected from the outline encompassing the footprint (**Figure 13b**). Intersections between the creation lines of planes B and D have been considered for this determination, as well as planes C and E at the lower level, i.e. the ground. These two points are sufficient to create the axis of articulation of the foot. A coordinate system R16(O16,x,y) is created at the end of this axis so that its X axis is on this axis of articulation (**Figure 13a**). Ball girth G1 is obtained with the XY cutting plane which is orientable along the X axis of R16 to detect the highest point of 1st metatarsal 8 (**Figure 13c**). The tibial metatarsal 2 and the metatarsal fibular 7 represent the extreme points on the G1 curve in the X and -X directions (towards the outside of the foot). The curve G'1 is a curve perpendicular to the ground aligned on the axis of articulation, representing the ball girth G'2 proposed by the 3D foot scanner.
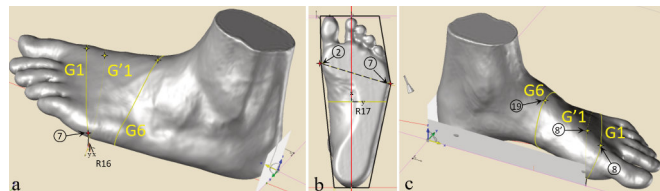
Figure 13: Detection of contact points 2, 7, 8, 19.

Mid-foot highest point (19)

The curve representing the girth at 50% foot length from the pternion is obtained from a cutting coordinate system R17(O17,x,y), located along the Brannock axis with the same method that was used for R8, R9, R10 (**Figure 13b**). On this curve, G6 detects the mid-foot highest point 19, which represents the extremum point in the direction of -Y (**Figure 13c**).

Medial malleolus (3), lateral malleolus (4)

The medial malleolus 3 and the lateral malleolus 4 are obtained respectively from two parallel planes B', C' to the planes B and C. For the second point, the second zone of contact has been taken into account, which is superior to the first (**Figure 14ab**).
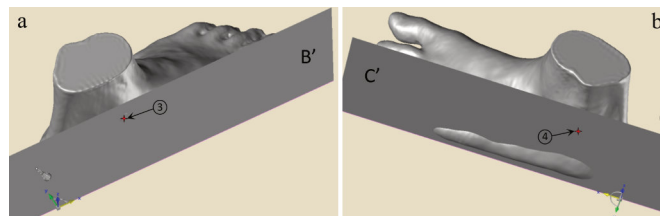
Figure 14: Detection of contact points 3, 4.

Sphyrion (9), sphyrion fibulare (10)

The detection of Sphyrion 9 and fibular sphyrion 10 uses a technique equivalent to points 3 and 4. The two detection planes B'', C'' move a little deeper in the foot to surround the malleolus. At this point, it is possible to create two curves surrounding each malleolus by locating the intersection between these two planes and the foot. The Sphyrion 9 and the fibulare sphyrion 10 are then at the lowest point of these, representing the extremum in -Z.
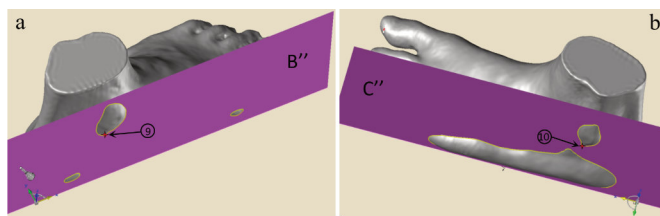
Figure 15: Detection of contact points 9, 10.

4.3 Measurement process analysis

The set of measurements necessary for the dimensioning of the foot was calculated from the anthopometric points and morphological curves that were detected and created by the 3D graphical process (**Table 1**: L1 to G6). **Table 1** compares the results obtained by the proposed method and the method used by the scanner. Since the scanner offers other

complementary measures (italic measurements) to the standard measures (scanner-specific terminology), these have been added to the list (L8 to A1) so that the comparison is complete.

The results show that all the foot sizing measures contain a very small error. Only the H5 measurement has a defect, mainly from the scanned measurement. Since this depends on the positioning of the patch that has been glued to the foot of the scanned person to locate the fibulare sphyrion, imprecision is naturally generated by this manual mode. The same problem occurred for H7 (patches positioned manually).

Since the scanner does not measure G as specified in the scientific bibliography (now G' for the scanner), point 8 has become a point 8' for the scanner, which explains this difference for H8. This difference is strongly reduced if the measurements are taken as practiced by the scanner (measures between parentheses for the 3D graphical process).

The measurement of the two angles is highly critical in the case of the scanner. This measurement is very important for defining the basic shape of the insole, and it depends on the outline encompassing the footprint.

Our measurement technique is based on the 3D foot shape, whereas the technique used by the scanner is different and is based on the line of the heel, thus leading to often negative angles.

Table 1 Measurement differences between 3D graphical and scan measurement.

	3D graphical measurement	Scan Measurement	Error (%)
L1 - Foot	277.5	280.6	1.1
L2 - Arch	200.6	203.4	1.3
L3 - Heel to medial malleolus	68.1		
L4 - Heel to lateral malleolus	41.3		
L5 - Heel to fifth toe	229.6		
L6 - Heel to Sphyrion	63.2		
L7 - Heel to Sphyrion fibulare	50.1		
H1 - Medial malleolus	92.0		
H2 - Lateral malleolus	79.2		
H3 - Instep	77.9	75.9	2.6
H4 - Sphyrion	65.5	67.8	3.3
H5 - Sphyrion fibulare	63.4	*78.3*	*21.7*
H6 - Mid-foot	75.2		
W1 - Foot	110.6		
W2 - Bimalleolar	70.8		
W3 - Mid-foot	95.2		
W4 - Heel	68.1	67.2	1.3
G1 - Ball	276.9 (277.5)	278.7	0.6
G2 - Instep	273.0 (267.7)	282.7	3.4
G3 - Long heel	372.0		
G4 - Short heel	353.2		
G5 - Ankle	272.3		
G6 - 50% foot length	266.7		
L8 - Fibulare instep	*166.6*	*175.7*	*5.1*
H7 - Arch or Navicular	*29.9*	*38.6*	*22.5*
H8 - Top of 1st metatarsal	*26.4 (53.2)*	*47.6*	*44.5 (11.7)*
W5 - Foot breadth	*115.9*	*115*	*0.7*
A1 - Toe 1st	*5°*	*-8.4°*	*159*
A1 - Toe 5st	*21.4°*	*4.9°*	*336*

5. Conclusion

This paper presents the 3D graphical process, which has been developed to detect the anthropometric points of the foot. These anthropometric points are crucial to obtain all the measurements characterizing the foot shape and dimensions. This non-contact measurement method proposes a tracking technique using virtual adjustable planes.

The results were compared with the industrial measurement data from specific software and the 3D foot scanner. The overall results show a good match between the data measured with the 3D scanner and our process. However, the industrial methods are very commentable because they depend on the positioning of the markers on the foot and anthropometric ratios integrated into the measurement process. This explains the few differences in some measures. Among other things, the use of anthropometric reports is undesirable and can lead to even more errors if the measured foot is out of the ordinary, i.e. with non-negligible

deformations. The advantage of our method is the ability to adapt to this problem, because it can be applied to feet with hallux valgus or hammertoe deformities commonly encountered during measurement campaigns, as discussed in further publications.

6. References

[1] Centre Hospitalier, "Le pied," Bois de l'abbaye. .

[2] J. A. DeBello, K. I. DeCoteau, and E. Beatty, "Taking A Novel Approach To Hammertoe Surgery," Podiatry Today, 2006. .

[3] E. B. Neves, A. J. Almeida, C. Rosa, J. Vilaca-Alves, V. M. Reis, and R. Mendes, "Anthropometric profile and diabetic foot risk: a cross-sectional study using thermography," pp. 1–3, 2016.

[4] S. K. van de Velde, M. Cashin, R. Johari, R. Blackshaw, A. Khot, and H. K. Graham, "Symptomatic hallux valgus and dorsal bunion in adolescents with cerebral palsy: clinical and biomechanical factors," Dev. Med. Child Neurol., vol. 60, no. 6, pp. 624–628, 2018.

[5] "Hallux valgus: only the handicap leads to the operation of the onion - Why Doctor," Pourquoidoctteur.fr, 2016. [Online]. Available: https://www.pourquoidocteur.fr/MaladiesPkoidoc/1126-Hallux-valgus-seul-le-handicap-conduit-a-l-operation-de-l-oignon. [Accessed: 19-Jun-2019].

[6] S. Taş and A. Çetin, "Mechanical properties and morphologic features of intrinsic foot muscles and plantar fascia in individuals with hallux valgus," Acta Orthop. Traumatol. Turc., no. xxxx, pp. 3–7, 2019.

[7] J. Ragland, "How to get rid of bunions," Getridofthings. .

[8] R. O. N. B. Killian, G. S. Nishimoto, and J. C. Page, "Fo an an," vol. 88, no. 8, pp. 365–374, 1998.

[9] A. Paiva de Castro, J. R. Rebelatto, and T. R. Aurichio, "The relationship between foot pain, anthropometric variables and footwear among older people," Appl. Ergon., vol. 41, no. 1, pp. 93–97, 2010.

[10] K. J. Mickle and C. J. Nester, "Morphology of the Toe Flexor Muscles in Older Adults With Toe Deformities," Arthritis Care Res., vol. 70, no. 6, pp. 902–907, 2018.

[11] A. Ladhani, "What are heel spurs?," step-by-step foot care, 2015. [Online]. Available: https://stepbystepfootcare.com/blog/what-are-heel-spurs/. [Accessed: 21-Jun-2019].

[12] U. Chundru, A. Liebeskind, F. Seidelmann, J. Fogel, P. Franklin, and J. Beltran, "Plantar fasciitis and calcaneal spur formation are associated with abductor digiti minimi atrophy on MRI of the foot," Skeletal Radiol., vol. 37, no. 6, pp. 505–510, Jun. 2008.

[13] H. Lemont, K. M. Ammirati, and N. Usen, "Plantar fasciitis: a degenerative process (fasciosis) without inflammation.," J. Am. Podiatr. Med. Assoc., vol. 93, no. 3, pp. 234–7, 2003.

[14] L. Özgönenel, "Plantar Fasciitis," Tech. Foot Ankle Surg., vol. 12, no. 2, p. 109, 2013.

[15] J. D.B., Hollinshead's Functional Anatomy of the Limbs and Back. Elsevier Health Sciences, 2008.

[16] T. F. Novacheck, "Review Paper The biomechanics of running," Gait Posture, vol. 7, pp. 77–95, 1998.

[17] "Foot pain | Mast Cells & Collagen Behaving Badly." .

[18] J. G. Atwater, "Cavus Foot (High-Arched Foot) Video | Orthopedic Doctor in Vero Beach, Florida." .

[19] G. Gijon-Nogueron, J. Montes-Alguacil, P. Alfageme-Garcia, J. A. Cervera-Marin, J. M. Morales-Asencio, and A. Martinez-Nova, "Establishing normative foot posture index values for the paediatric population: a cross-sectional study," J. Foot Ankle Res., vol. 9, no. 1, p. 24, Dec. 2016.

[20] D. Carmody, P. Bubra, G. Keighley, and S. Rateesh, "Posterior tibial tendon dysfunction: An overlooked cause of foot deformity," J. Fam. Med. Prim. Care, vol. 4, no. 1, p. 26, 2015.

[21] D. S. Williams, I. S. McClay, J. Hamill, and T. S. Buchanan, "Lower extremity kinematic and kinetic differences in runners with high and low arches," J. Appl. Biomech., vol. 17, no. 2, pp. 153–163, 2001.

[22] M. Birtane and H. Tuna, "The evaluation of plantar pressure distribution in obese and non-obese adults," Clin. Biomech., vol. 19, no. 10, pp. 1055–1059, 2004.

[23] S. A. Vela, L. A. Lavery, D. G. Armstrong, and A. A. Anaim, "The

effect of increased weight on peak pressures: Implications for obesity and diabetic foot pathology," J. Foot Ankle Surg., vol. 37, no. 5, pp. 416–420, 1998.

[24] M. Voracek, M. L. Fisher, B. Rupp, D. Lucas, and D. M. T. Fessler, "Sex Differences in Relative Foot Length and Perceived Attractiveness of Female Feet: Relationships among Anthropometry, Physique, and Preference Ratings. Perceptual and Motor Skills," 2007.

[25] Printerest, "Ankle anatomy." .

[26] A. Cichocka, P. Bruniaux, and I. Frydrych, "3D Garment Modelling - Creation of a virtual mannequin of the human body," Fibres Text. East. Eur., vol. 22, no. 6, pp. 123–131, 2014.

[27] C. P. Witana, S. Xiong, J. Zhao, and R. S. Goonetilleke, "Foot measurements from three-dimensional scans: A comparison and evaluation of different methods," Int. J. Ind. Ergon., vol. 36, no. 9, pp. 789–807, 2006.

[28] M. Hajaghazadeh, R. Emamgholizadeh Minaei, T. Allahyari, and H. Khalkhali, "Anthropometric Dimensions of Foot in Northwestern Iran and Comparison with Other Populations," Heal. Scope, vol. 7, no. 3, 2018.

[29] M. Pantazi, A. M. Vasilescu, A. Mihai, and D. Gurau, "Statistical-mathematical processing of anthropometric foot parameters and establishing simple and multiple correlations. Part 1: statistical analysis of foot size parameters," Leather Footwear J., vol. 17, no. 4, pp. 199–208, Dec. 2017.

[30] Y.-C. C. Lee, G. Lin, and M.-J. J. J. Wang, "Comparing 3D foot scanning with conventional measurement methods.," J. Foot Ankle Res., vol. 7, no. 1, p. 44, 2014.

[31] D. Webb, D. V. Bernardo, and T. Hermenegildo, "Evaluating and Improving Footprint Measurement : Orientation and Lengths," Anthropologie, pp. 277–287, 2006.

[32] T. G. McPoil, B. Vicenzino, M. W. Cornwall, and N. Collins, "Can foot anthropometric measurements predict dynamic plantar surface contact area?," J. Foot Ankle Res., vol. 2, no. 1, 2009.

[33] O. Vrdoljak, M. K. Tiljak, and M. Čimić, "Anthropometric measurements of foot length and shape in children 2 to 7 years of age," Period. Biol., vol. 119, no. 2, pp. 125–129, 2017.

[34] K. Hasanzadeh and K. Salehzadeh, "The Relationship between Anthropometric Indices in Children and their Kinetic Performances of Agility , Balance and Foot Power The Relationship between Anthropometric Indices in Children and their Kinetic Performances of Agility , Balance and Foot Power," no. May 2015, 2016.

[35] "BFTS GmbH." .

[36] B. Nácher et al., "A footwear fit classification model based on anthropometric data," SAE Tech. Pap., vol. 1, no. May 2014, 2006.

[37] "Boite ſ empreintes double - Salembier Pédicurie Podologie." .